

# Reducing Ultrafine Particle Emissions Using Air Injection in Wood-Burning Cookstoves

*Vi H. Rapp†\*, Julien J. Caubel†‡, Daniel L. Wilson†‡, Ashok J. Gadgil†¶*

† Environmental Technologies Area, Lawrence Berkeley National Laboratory, Berkeley,  
California 94720, United States

‡ Department of Mechanical Engineering, University of California, Berkeley, Berkeley,  
California 94720, United States

¶ Department of Civil and Environmental Engineering, University of California, Berkeley,  
Berkeley, California 94720, United States

\*1 Cyclotron Road MS 90R2121, Berkeley, CA 94720

Phone: 01-510-495-2035; Fax: 01-510-486-4089; E-mail: vhrapp@lbl.gov

**Accepted June 2016 to Environmental Science and Technology**

**DOI: 10.1021/acs.est.6b01333**

## ABSTRACT

In order to address the health risks and climate impacts associated with pollution from cooking on biomass fires, researchers have focused on designing new cookstoves that improve cooking performance and reduce harmful emissions, specifically particulate matter (PM). One method for improving cooking performance and reducing emissions is using air injection to increase turbulence of unburned gases in the combustion zone. Although air injection reduces total PM mass emissions, the effect on PM size-distribution and number concentration has not been thoroughly investigated. Using two new wood-burning cookstove designs from Lawrence Berkeley National Laboratory, this research explores the effect of air injection on cooking performance, PM and gaseous emissions, and PM size distribution and number concentration. Both cookstoves were created using the Berkeley-Darfur Stove as the base platform to isolate the effects of air injection. The thermal performance, gaseous emissions, PM mass emissions, and particle concentrations (ranging from 5 nm to 10  $\mu\text{m}$  in diameter) of the cookstoves were measured during multiple high-power cooking tests. The results indicate that air injection improves cookstove performance and reduces total PM mass but increases total ultrafine (less than 100 nm in diameter) PM concentration over the course of high-power cooking.



## INTRODUCTION

One of the world's greatest environmental health risk factors is exposure to emissions from cooking with solid biomass fuels; approximately 4 million premature deaths per year are

attributed to this practice.<sup>1-3</sup> Additionally, the widespread use of cooking with solid biomass fuel contributes to climate change through increased emissions of carbon dioxide and black carbon, particulates that strongly absorb solar radiation.<sup>4</sup> Researchers have explored new environmental technologies for increasing efficiency in biomass cookstoves while decreasing harmful emissions, primarily focusing on particulate matter (PM).<sup>5-11</sup> Previous research reveals that introducing turbulence (via air injection) into the gas-phase combustion zone can dramatically improve cooking performance and reduce the total mass of PM generated from biomass combustion.<sup>5,9,11</sup> Injecting air into the gas-phase combustion zone to generate turbulence (here-on referred to as air injection) promotes better gaseous fuel-air mixing, leading to more complete combustion, and can increase residence time of soot in the flame, promoting oxidation of soot.<sup>12</sup>

Although air injection can decrease total PM mass emitted, it is unclear if this technique reduces the number concentration of all PM emission sizes uniformly and may concurrently increase the number of ultrafine particles per mass of fuel burned, which may be more harmful to human health.<sup>6,13</sup> If total number of ultrafine particles per meal shifts to emit more particles smaller than 50 nm in diameter, then the total deposition of these ultrafine particles is expected to increase in all three primary lung regions: nasal pharyngeal, bronchial, and alveolar. Several researchers<sup>14-18</sup> show that particles smaller than 50 nm in diameter exhibit strong cytotoxicity in lung tissue including oxidative DNA damage and proinflammatory response. These effects are observed over a range of particle chemistries, but the most deleterious effects are typically observed with ultrafine particles of combustion origin. These studies show that cytotoxicity of particles on a per-mass basis is typically inversely related to the size of the particles, pointing to the increased toxicity of ultrafine aerosols.

A few researchers have measured ultrafine particle size distributions from improved stoves, but few of the tested stoves incorporate air injection.<sup>5,6</sup> For example, Jetter et al.<sup>5</sup> measured emission factors of ultrafine particles for multiple cookstoves, including four forced-draft cookstoves, and found that the forced-draft stoves produced less total particulate mass but increased total ultrafine particle emission factors per useful energy delivered to the pot. However, the size distribution of the particles was not measured. Just et al.<sup>6</sup> measured ultrafine particle number concentrations and size distributions from a three-stone fire, a natural draft rocket stove, and a natural draft gasifier stove operating under “steady” conditions at a medium-power similar to a simmer. They also found that the improved stoves produced less total particulate mass, but increased quantities of smaller particles with diameters smaller than 30 nm. However, none of the stoves tested incorporated air injection and the testing conditions were not representative of an actual cooking event or a complete burn cycle.

In this paper, we investigate the impact of air injection on biomass cookstove performance and emissions using two new stoves designed by Lawrence Berkeley National Laboratory. Both stove designs were created using the wood-burning Berkeley-Darfur Stove as the base platform in order to isolate the effects of air injection on performance and emissions. The thermal performance, gaseous emissions, PM mass and number concentration, and PM size-distribution (ranging from 5 nm to 10  $\mu\text{m}$  in diameter) of the cookstoves were measured during multiple high-power tests. The high-power tests were conducted at a constant firepower and include both startup and steady-state emissions as room temperature water is brought to a boil (cold start phase of the Water Boiling Test 4.3.2<sup>19</sup>). Performance and emission results from the air injection stoves are compared to the base platform, Berkeley-Darfur Stove (BDS), and a three-stone fire (TSF).

## MATERIALS AND METHODS

**Berkeley Air Injection Cookstove Designs.** The air injection cookstoves were designed to investigate the scientific underpinnings for significantly reducing particulate matter (PM) emissions from front-loading, wood-burning cookstoves. In order to parametrically study the effects of air injection and identify key parameters that significantly reduce PM emissions, we used the Berkeley-Darfur Stove (BDS) as the base platform for all air injection cookstove designs in this study. The BDS was chosen as the base platform because it was developed by Lawrence Berkeley National Laboratory and has been fully tested and characterized by different researchers in various experimental conditions.<sup>5,7</sup> This robust characterization data increases certainty when identifying the effects of air injection on cooking performance and emissions. Both air injection cookstoves were designed and constructed for laboratory testing. Final field designs will be more user-friendly and cost effective than the research designs described below.

The Berkeley Umbrella Stove (BUS), Figure 1, incorporates an umbrella-shaped air injection manifold into the BDS firebox with downward-facing jets that promote mixing and complete combustion. During operation, compressed air from a cylinder was regulated using a 2-stage regulator and then flowed through a rotameter (measuring volumetric flow rate) before passing through the central column into the umbrella-shaped manifold. For field use, a fan powered by the stove's heat (e.g. thermoelectric generator) or by a rechargeable battery could supply air to the umbrella manifold, which was designed for operation with a small blower. Additional design specifications for the BUS can be found in the SI.

When designing the BUS, it was understood that the umbrella acts as an undesirable radiation shield between the fire and the pot, thereby somewhat reducing heat transfer efficiency.

However, we still expected an overall reduction in emissions per task due to the addition of preheated air injection.

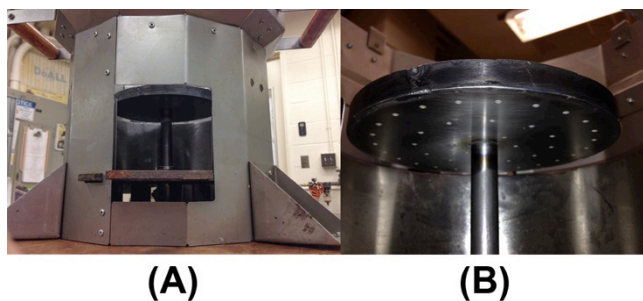


**Figure 1.** The Berkeley Umbrella Stove. Front view (A) shows the central column that provides air to the umbrella manifold. Inside view (B) shows the 42 1/8-inch (3.175 mm) holes evenly distributed on the bottom surface that inject air into the gas-phase combustion zone in the firebox.

The Berkeley Shower Stove (BSS) incorporates a manifold that is located below the stove grate and employs up to eight interchangeable stainless-steel nozzles, or “shower-heads,” to inject air over the firebox wall into the combustion zone (see Figure 2). Before reaching the manifold and nozzles, air travels through coiled copper tubing located directly below the grate to preheat the air, as shown in Figure 2(A). The circular steel manifold also serves to transfer heat from the combustion process above to the injected air.

The BSS avoids the radiation shielding effect associated with the BUS and enables rapid, parametric identification of air injection geometries that improve thermal performance while significantly reducing emissions. The following parameters on the BSS can be quickly and easily modified for parametric investigation: (1) the total number of nozzles, (2) the orientation of nozzles, (3) the height of the nozzles above the grate, and (4) the air injection flow rate. Because the BSS was designed for rapid parametric studies, the manifold design was not optimized to operate with a blower and uses the same air supply system described for the BUS. However, the

design could be optimized with a less restrictive air injection system for use with a blower. Additional design specifications for the BSS can be found in the SI.

In this study, eight stainless steel nozzles were used for air injection. The six nozzles closest to the fuel magazine feed are oriented radially toward the center of the grate while the two nozzles at the rear of the firebox are angled toward each other to prevent hot gases and flames from exiting out the fuel feed toward the stove operator. All nozzle tips are angled approximately 45° downward from the horizontal plane of the grate. This optimal configuration was chosen using preliminary experimental results.

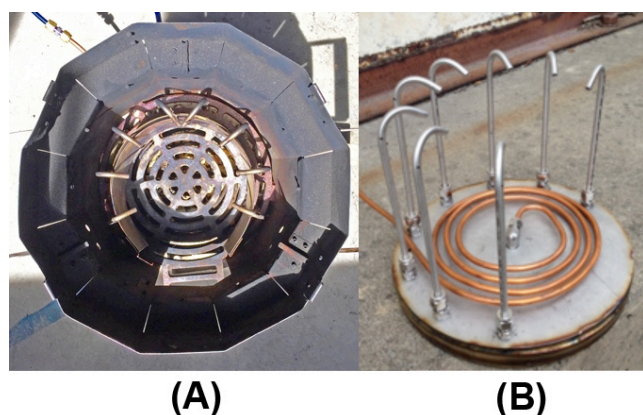


**Figure 2.** The Berkeley Shower Stove. The top view (A) shows the nozzles protruding through the stove grate to inject air over the firebox into the gas-phase combustion zone. The air manifold (B) sits below the grate. Air is preheated through the copper tubing before entering the manifold and being distributed to the 8 nozzles.

**Experimental Setup.** All experiments were conducted in the Lawrence Berkeley National Laboratory cookstove research facility. A schematic of the cookstove research facility and equipment is shown in Figure 3. Pollutants from the stove were captured by an exhaust hood and transported outside the building through an exhaust duct system. Pollutants were sampled in the exhaust duct before exiting the building. The volumetric flow rate in the exhaust duct is 400

m<sup>3</sup>/hr (235 CFM), which represents 10 air exchanges per hour in a 40 m<sup>3</sup> kitchen –within the observed range cited by the World Health Organization’s Indoor Air Quality Guidelines<sup>3</sup>. The volumetric flow rate in the exhaust duct was determined using a real-time measurement of the pressure drop across a calibrated orifice, shown in Figure 3.

Carbon monoxide (CO), carbon dioxide (CO<sub>2</sub>), and oxygen (O<sub>2</sub>), volume concentrations were measured using a California Analytical Instruments (CAI) 600 Series nondispersive infrared absorption spectroscopy (NDIR) analyzer. Total PM<sub>2.5</sub> mass was measured gravimetrically by sampling exhaust gas from the duct and passing it through an ultra-sharp cutoff PM<sub>2.5</sub> cyclone to remove particles larger than 2.5 μm (BGI instruments). A precision, 16.7 LPM critical orifice controls flow through the cyclone. Particles smaller than 2.5 μm are deposited on a Teflon filter that is humidity conditioned and weighed on a calibrated microbalance both before and after each experiment. The difference in mass of the filter before and after testing yields the total PM<sub>2.5</sub> mass emission per high-power test.

Particle number concentration and size distribution ranging from 5 nm to 10 μm were measured at 1 Hz sampling rate using a TSI 3330 Optical Particle Sizer (OPS) and a TSI 3091 Fast Mobility Particle Sizer (FMPS). The OPS requires the refractive index of measured particles to be set externally and was set to 1.57 based on previous research that measures the refractive index for Douglas fir as a primary fuel wood.<sup>20,21</sup> Prior to reaching the instruments, the real-time aerosol sample, which leads to the FMPS and OPS, was diluted with a compressed cylinder of ultra zero air (O<sub>2</sub> 19.5% - 23.5%, water < 2 ppm, hydrocarbons < 0.1 ppm, CO<sub>2</sub> < 0.5 ppm, CO < 0.5 ppm) to increase measurement accuracy and prevent frequent maintenance of the instruments. The dilution ratio for the real-time aerosol sample line was determined using exhaust sample flow rates and by comparing measured CO<sub>2</sub> before and after dilution. Ambient

and diluted CO<sub>2</sub> volume concentrations were measured with a PP Systems SBA-5 NDIR gas analyzer.

At the beginning and end of each experiment day, all instruments were checked for calibration to ensure accuracy. Prior to each high-power test, stoves and pots were scrubbed clean to avoid accumulation of soot and tar that could impact heat transfer in successive replicate tests. Further details for the experimental setup and equipment are provided in the SI.

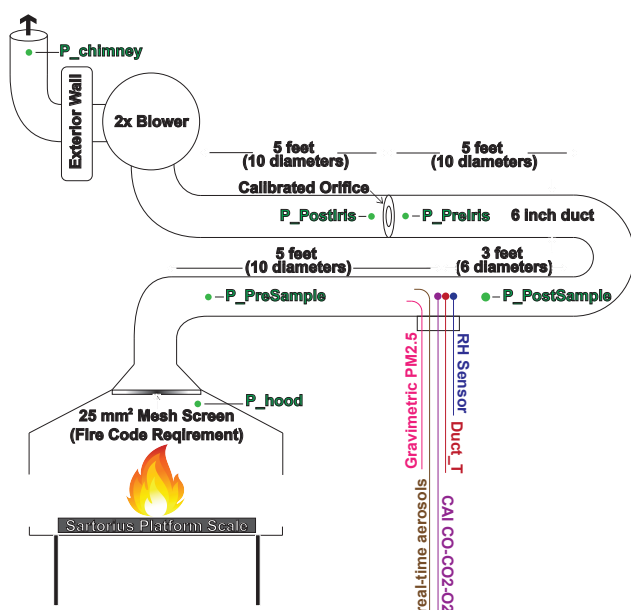


**Figure 3.** Schematic of the Lawrence Berkeley National Laboratory cookstove research testing facility.

**Experimental Procedure.** A total of 34 high-power tests were conducted: ten each on the TSF, the BDS, and the BUS, and four on the BSS. These multiple replicate tests were conducted to ensure adequately tight confidence intervals on the mean values of stove performance and emission metrics. Each high-power test follows procedures for the cold start phase described in the Water Boiling Test (WBT) 4.2.3,<sup>19</sup> where 5 L of room temperature water is brought to boil. Since the manufactured stoves in this study are intended for use with a Darfuri-style pot, all tests

were conducted using a 1.7 kg round-bottomed aluminum Darfuri pot,<sup>5</sup> which is not specified by the WBT 4.2.3<sup>19</sup> protocol.

The fire was started using untreated pine wood shavings and Douglas-fir kindling. The fire was then built up by adding Douglas-fir fuel-wood pieces to heat the water from ambient temperature to boiling (approximately 99°C for experiments presented in this paper). Both the kindling and the fuel-wood were untreated and harvested from a single Douglas-fir tree and stored in a dry location for at least 1 year prior to the experiments. The moisture content of the wood ranged from 7% to 9% on a wet basis.

All stoves were tested at a fuel feed rate that maintained a constant CO<sub>2</sub> emission rate and in turn a constant firepower. Maintaining a constant firepower allows for immediate performance and emissions comparisons between the stoves. Due to the unstable nature of the TSF and its low efficiency, maintaining a steady lower firepower that was optimal for the manufactured stoves (~2 kW) was extremely challenging and did not result in successfully boiling the water. Therefore, a higher firepower (~5 kW), and corresponding CO<sub>2</sub> concentration, were chosen for testing the TSF and the three engineered stoves to ensure a consistent firepower could be maintained over the duration of an individual test and that the test successfully boiled water. Using duct CO<sub>2</sub> concentration as an indication of firepower also ensured that each test was accurately replicated.

Upon completion of each test, the unburned wood and char were weighed. Gaseous and particle emissions data were collected for the duration of all stove tests (from ignition until the water reached boiling temperature). In order to minimize instrument errors and avoid accelerating factory maintenance schedules caused by extended exposure to high-concentration

PM, real-time particle emissions data using the ultrafine particle analyzers (the TSI FMPS and OPS) were measured only for six of the ten tests conducted for the TSF and the BDS.

Preliminary tests were conducted on the BUS and BSS to identify the best air injection supply rate for minimizing production of PM<sub>2.5</sub> mass emissions. The start time for air injection was chosen to ensure the fire was well established to reduce the risk of quenching the fire. Preliminary testing of the BUS indicated that air injection could be started 3 minutes after ignition at a supply rate of 56.6 LPM (2 CFM) at a manifold pressure of ~490 Pa (0.07 psi). Preliminary testing of the BSS indicated that air injection could be started 2 minutes after ignition at a supply rate of 42.5 LPM (1.5 CFM) at a manifold pressure of ~17.2 kPa (2.5 psi). Due to the thermal mass of the umbrella, more time was required to establish a stable fire in the BUS before air injection could be initiated. For both the BUS and the BSS, air injection, measured using an inline rotameter, was supplied at a constant flow rate for the remainder of the cold start test.

**Data Analysis.** High-power test performance metrics such as firepower, thermal efficiency, and CO and PM<sub>2.5</sub> mass emissions (both reported in g/MJ delivered to the pot) are calculated using the methods reported for the cold start phase of the Water Boiling Test 4.3.2.<sup>19</sup> Additional performance and emissions calculations are provided in the SI. For all data, 95% confidence bounds are determined assuming a Student's t-distribution<sup>22</sup> using methods described by Wang et al. (2014).

## RESULTS AND DISCUSSION

**Performance Metrics.** Performance metrics for the operation of each stove during the high-power test are presented in Table 1. Performance emission metrics for CO and PM<sub>2.5</sub> are reported in mass per useful energy delivered to the pot. The results show that the addition of air injection

significantly reduces  $PM_{2.5}$  and CO mass emissions. Compared to the TSF, the BUS and the BSS reduce  $PM_{2.5}$  mass emissions by 35% and 66%, respectively. However, the BDS produces similar  $PM_{2.5}$  mass emissions to the TSF. In order to maintain the high (5.2 kW) firepower in the BDS, the firebox was packed with fuel-wood. Increasing the amount of fuel wood in the BDS's firebox obstructs the natural draft of primary air through the fuel grate and the fuel feed door from entering the combustion zone. Blocking the primary air flow reduces mixing and results in a fuel-rich flame that is quenched against the cold pot or with ambient air, causing the nucleation and growth of particles with larger diameter and mass. Figure 4 further supports this theory, showing that the BDS generates more particles of larger diameter (between 500 and 10000 nm) than the TSF. Increasing the primary air to the BDS by operating at a lower firepower can achieve better  $PM_{2.5}$  mass emissions results than the TSF (60 to 75% reduction), as shown by previous researchers.<sup>5,7</sup>

The results also show that CO mass emissions per energy delivered to the pot from the BUS are comparable to the BDS, and both produce about 30% to 40% less CO than the TSF. Previous research<sup>4</sup> reports the BDS producing 50% to 65% less CO than the TSF. This difference is likely due to the difference in reported thermal efficiencies and is discussed further in the following paragraph. The BSS shows additional improvements, producing about 70% less CO per test than the TSF.

Although the addition of air injection (deployed in BUS and BSS) reduced both  $PM_{2.5}$  and CO mass emissions per energy delivered to the pot, it did not significantly improve thermal efficiency or time to boil relative to the BDS. The BUS took approximately 4 minutes longer to boil water than the BDS, while the BSS boiled water in about the same amount of time as the BDS. Similarly, the BUS shows about a 15% decrease in thermal efficiency compared to the

BDS and BSS. Reported thermal efficiency for the BDS from Jetter et al. (2012), 37.4%, agrees well with the findings in this study, 34%. It should be noted that thermal efficiency for our well-tended TSF is about 23%, far above the 15% thermal efficiency reported by other researchers.<sup>5</sup> This difference in performance is likely due to the difference in pot material and shape used to conduct the TSF tests. We also recognize that the performance of a TSF is also highly dependent on the stove operator.

The BUS and BSS show improvements in modified combustion efficiency (MCE) compared to the TSF and BDS. The TSF and the BUS have an MCE around 96%, while the BUS and BSS have an MCE of almost 97% and 99%, respectively. These results agree well with previous research conducted on similar stoves.<sup>5-7</sup>

The stove performance results indicate that the addition of air injection can reduce  $PM_{2.5}$  and CO mass emissions per energy delivered to the pot for a high-power test, but an overall design optimization is required to simultaneously increase stove thermal efficiency and reduce time to boil. Although the BUS reduces  $PM_{2.5}$  mass emissions, the umbrella limits emissions reductions by quenching the flames and acting as a radiation shield that reduces heat transfer to the pot. The BSS, however, does not obstruct heat transfer to the pot, closely matching the thermal efficiency and time to boil of the BDS, while reducing  $PM_{2.5}$  mass emissions by 66% per high-power test. For all performance metrics, the BUS and BSS outperform the TSF.

**Table 1.** Calculated high-power test performance metrics of tested stoves using methods described for the cold start phase of the Water Boiling Test 4.3.2.<sup>19</sup> Values represent the mean of *n* tests with +/- indicating 95% confidence intervals, assuming Student's t-distribution.

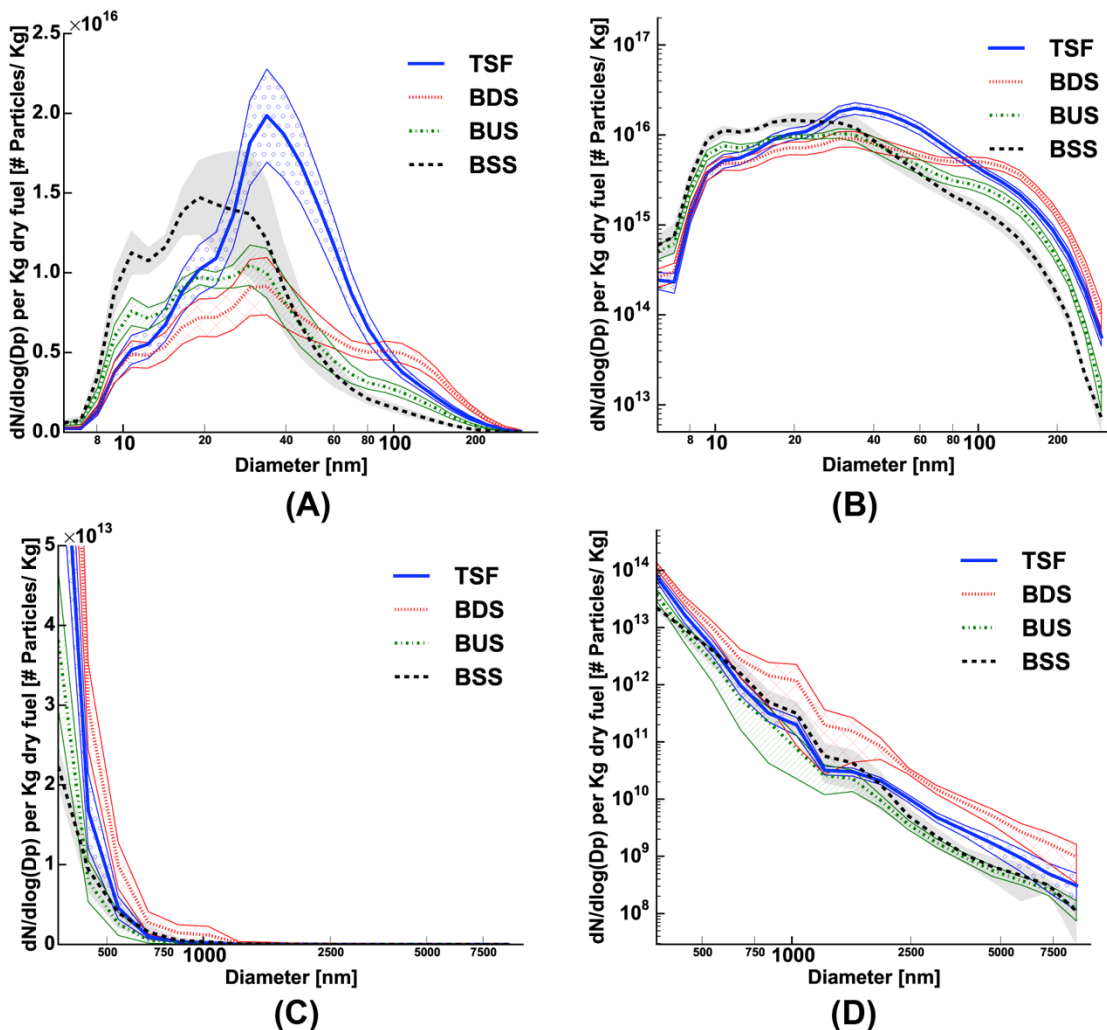
Stove Type	TSF ( <i>n</i> =10)	BDS ( <i>n</i> =10)	BUS ( <i>n</i> =10)	BSS ( <i>n</i> =4)
<b>Corrected Time to Boil [min]</b>	32 ± 4	18 ± 1	21 ± 1	18 ± 1
<b>Firepower [W]</b>	5294 ± 578	5200 ± 270	5390 ± 367	5203 ± 438
<b>Thermal Efficiency [%]</b>	23 ± 2	34 ± 1	29 ± 1	34 ± 1
<b>Modified Combustion Efficiency [%]</b>	96.3 ± 0.5	95.9 ± 0.7	96.9 ± 0.6	98.6 ± 0.5
<b>CO Emissions [g/MJ<sub>delivered</sub>]</b>	10 ± 2	7 ± 1	6 ± 1	3 ± 1
<b>PM<sub>2.5</sub> Emissions [mg/MJ<sub>delivered</sub>]</b>	692 ± 155	738 ± 85	455 ± 66	230 ± 52

**Fine and Ultrafine Particle Emissions.** The total number of ultrafine particles (measured by the FMPS) generated by each stove over the entire high-power test and normalized by equivalent dry fuel consumed (as calculated in the WBT 4.3.2<sup>19</sup>) is shown in Figures 4(A) and 4(B). The particle distribution for the BUS and BSS is bimodal, with the smaller diameter mode around 10 nm. This mode may be associated with the nucleation of volatile particles in flaming combustion, as the partially oxidized gas-phase fuel in the flame zone is cooled by the injected air.<sup>24,25</sup> The larger diameter mode is a result of aggregation<sup>24,25</sup> that occurs around 19 nm for the BSS, and around 29 nm for the BUS. The peak concentration for the BDS occurs around 34 nm, agreeing well with previous research.<sup>6</sup> In addition, the BDS demonstrates a secondary peak at 100 nm, which could be due to the aggregation of larger smoldering particles. The TSF has a peak

concentration around 40 nm that could be attributed to larger organic particles generation from smoldering.

Both the BUS and the BSS generate more ultrafine particles than the BDS for particles smaller than approximately 60 nm. The BUS and BSS also generate more ultrafine particles than the TSF for particles smaller than approximately 20 nm. For particle sizes around 10 nm, the BUS and BSS generate about 2.2 and 1.5 times more particles, respectively, than the BDS per kilogram of dry fuel for the high-power test. These results indicate that the addition of air injection may increase the total number of ultrafine particles compared to the same stove without air injection. Additionally, the stove designs with air injection generate more ultrafine particles smaller than 20 nm than the TSF per kilogram of dry fuel.

For particles larger than 300 nm, shown in Figure 4, the TSF and BDS generate more particles per kilogram of dry fuel than the BUS and the BSS. It should be noted that none of the stoves produced enough particles near the 10000 nm range for the OPS to measure accurately.



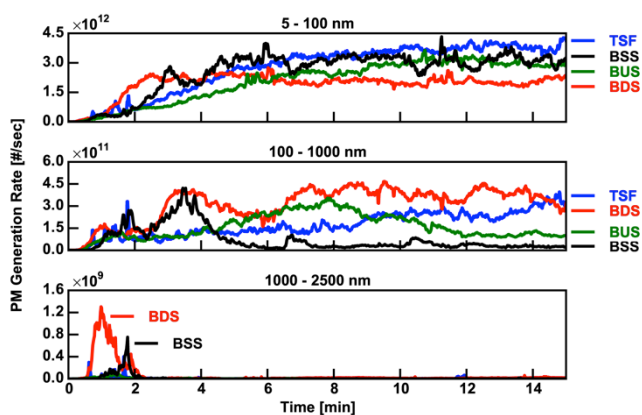
**Figure 4.** Fine and ultrafine particle concentration per kilogram of dry fuel consumed during the high-power test (cold start phase of the Water Boiling Test 4.3.2<sup>19</sup>) measured by the FMPS (A and B) and the OPS (C and D) plotted on a normal-log scale (left) and a log-log scale (right). Shaded regions represent 95% confidence bounds for each size bin.

Figure 5 shows the average particle generation rates from the TSF, BDS, BUS, and BSS, during the first 15 minutes of the high-power test. The particles are grouped into three size ranges: 5-100 nm, 100-1000 nm, and 1000-2500 nm. Figure 5 shows that almost all of the fine particles between 1000 and 2500 nm are generated during the first three minutes after ignition, when both the wood and the stove are cold. After ignition, the cold conditions reduce the flame

temperature resulting in incomplete combustion and greater escape of volatile gases from the flame zone owing to slower oxidation kinetics. These gases readily nucleate and grow , increasing the production of larger particles.<sup>26</sup> As the stove and the wood temperatures increase, after about 3 minutes, the generation of particles larger than 1000 nm rapidly decreases, due to combustion of more volatile gases and reduced nucleation, while particles smaller than 100 nm steadily increase until the steady state at approximately 7 minutes.

For the TSF, the emissions rate of particles ranging from 100 to 1000 nm steadily increases for the duration of the test. Particle emission rate for the BDS increases for the first 7 minutes and then levels off for the remainder of the test. Particles in the same range decrease after 5 minutes of operation for the BSS and after 10 minutes of operation for the BUS. After ignition, the manifolds in both the BUS and the BSS are at room temperature, and initially inject room temperature air into the firebox. The injection of cool air, relative to the fire temperature, effectively quenches the combustion process and drives the growth of accumulation mode particles,<sup>26</sup> peaking at roughly 3 and 8 minutes of operation for the BSS and BUS, respectively. However, once the manifolds reach steady-state temperatures, the air injected is heated and enables complete combustion of volatile gases, thus decreasing particle generation in this size range. The additional time required to decrease the particle generation rate for the BUS is likely due to the additional energy required to heat the umbrella manifold, which lowers the temperature in the firebox and quenches the flame. The BSS reduces particles in this range earlier than both the BUS and the BDS because it is fitted with a copper coil under the grate to increase heat transfer to the airflow prior to injection and has insignificant thermal mass in the firebox. After the stoves reach a steady operating temperature, the BDS and the TSF generate more particles than the BUS and BSS, with the BSS generating the least.

The particle range with the largest generation rate is 5 to 100 nm. In this range, the particle generation rate is similar for all four stoves when operated at approximately the same fuel-burning rate. However, it is important to note that some stoves deliver the same cooking power (useful energy delivered per time) at lower fuel-burning rates, leading to lower total particle number emissions in the same size range. After the first 5 minutes of operation, when the stoves reach a steady operating temperature, the generation rate of the TSF is comparable to the BUS and the BSS, while the BDS generates the least amount of particles in this range. A possible explanation for the elevated BUS and BSS generation rates is that the air injection aids in creating an environment where fewer accumulation mode particles exist, producing less surface area for condensation and growth<sup>5</sup>. Figure 4 supports this theory as the peak emission factors occur for particles with a geometric mean diameter less than 20 nm. The TSF, however, exhibits higher emission factors for particles with a geometric mean diameter around 40 nm, which is possibly due to larger organics from smoldering.



**Figure 5.** Average particle generation rate from the first 15 minutes of testing the TSF, BDS, BUS, and BSS. Particle sizes are divided into ranges from 5 to 100 nm, 100 to 1000 nm, and 1000 to 2500 nm. During one of the BDS experiments, a piece of wood added during the first 2 minutes of operation contained sap, thus generating a spike in the 1000 to 2500 nm range.

The results from this study show that air injection may increase the generation of particles smaller than 50 nm in diameter. The resulting shift in geometric mean diameter of particles toward the ultrafine particles may adversely impact health since total deposition of these ultrafine particles would increase in all three primary lung regions.<sup>14-18</sup> Deposition of particles smaller than 10 nm would increase in the nasal and bronchial regions. In the alveolar region, deposition of particles between 10 and 50 nm would increase because these particles lack the diffusivity to deposit higher in the respiratory tract.<sup>27</sup> This is especially concerning for the BSS, which emits significantly more particles in this size range than the other stoves.

This research investigated the performance and emissions of two wood burning air-injection cookstoves designed by LBNL. The results show that air injection can reduce PM<sub>2.5</sub> mass emissions per energy delivered to the pot but may generate more ultra fine particles between 5 and 50 nm during a high-power test. The most efficient air-injection stove produced the least PM<sub>2.5</sub> mass but generated more ultra fine particles smaller than 30 nm than the other two engineered stoves (BDS and BUS) and the TSF. As more air-injection stoves are disseminated to the field, additional research is required to ensure the new and improved stove designs not only improve boiling time and thermal efficiency, but also protect health by reducing fine and ultrafine particle mass and number concentrations. Reductions in particulate mass and number concentrations could be achieved by (1) limiting the thermal mass of the manifold, (2) allowing for greater preheating of injected air, (3) increasing turbulent mixing inside the combustion zone, and (4) increasing the residence time of the exhaust gases in the combustion zone. However, additional research is needed to better understand the effects of each of these modifications on different stove types (e.g. charcoal, pellet).

Presently, there are no United States Environmental Protection Agency regulations, World Health Organization guidelines, or International Organization for Standardization/International Workshop Agreement standards in place for regulating ultrafine particle number concentrations. However, the European Union vehicle emissions legislation regulates and limits both particle mass and particle number.

#### SUPPORTING INFORMATION

Additional information on the stove designs, experimental setup, and results are available in the Supporting Information. This material is available free of charge via the Internet at <http://pubs.acs.org/>.

#### ACKNOWLEDGMENT

This work was performed at the Lawrence Berkeley National Laboratory, operated by the University of California, under DOE Contract DE-AC02-05CH11231. We gratefully acknowledge support from DOE's Biomass Energy Technologies Office. Authors J.J.C. and D.L.W. were supported by National Science Foundation's Graduate Research Fellowship Program. The authors also acknowledge Tom Kirchstetter, Kathleen Lask, Sharon Chen, and Yannick Sarrand for their support with this research.

#### ABBREVIATIONS

BDS, Berkeley-Darfur Stove; BSS, Berkeley Shower Stove; BUS, Berkeley Umbrella Stove; CAI, California Analytical Instruments; CO<sub>2</sub>, Carbon Dioxide; CO, Carbon Monoxide; LBNL, Lawrence Berkeley National Laboratory; MCE, Modified Combustion Efficiency; NIOSH, National Institute for Occupational Safety and Health; PM, Particulate Matter; PM<sub>2.5</sub>, Particulate

Matter with an aerodynamic diameter less than or equal to 2.5  $\mu\text{m}$ ; ppmv, Parts per Million by Volume; TSF, Three Stone Fire.

## REFERENCES

- (1) Vos, T.; Barber, R. M.; Bell, B.; Bertozzi-Villa, A.; Biryukov, S.; Bolliger, I.; Charlson, F.; Davis, A.; Degenhardt, L.; Dicker, D.; et al. Articles Global, regional, and national incidence, prevalence, and years lived with disability for 301 acute and chronic diseases and injuries in 188 countries, 1990–2013: a systematic analysis for the Global Burden of Disease Study 2013. *The Lancet* **2015**, *386* (9995), 743–800.
- (2) Smith, K. R.; Bruce, N.; Balakrishnan, K.; Adair-Rohani, H.; Balmes, J.; Chafe, Z.; Dherani, M.; Hosgood, H. D.; Mehta, S.; Pope, D.; et al. Millions Dead: How Do We Know and What Does It Mean? Methods Used in the Comparative Risk Assessment of Household Air Pollution. *Annu. Rev. Public. Health.* **2014**, *35* (1), 185–206.
- (3) World Health Organization. *WHO Guidelines for Indoor Air Quality*; WHO Document Production Services: Geneva, Switzerland, 2014; pp 1–172.
- (4) Bond, T. C.; Doherty, S. J.; Fahey, D. W.; Forster, P. M.; Berntsen, T.; DeAngelo, B. J.; Flanner, M. G.; Ghan, S.; Kärcher, B.; Koch, D.; et al. Bounding the role of black carbon in the climate system: A scientific assessment. *J. Geophys. Res. Atmos.* **2013**, *118* (11), 5380–5552.
- (5) Jetter, J.; Zhao, Y.; Smith, K. R.; Khan, B.; Yelverton, T.; DeCarlo, P.; Hays, M. D. Pollutant Emissions and Energy Efficiency under Controlled Conditions for Household Biomass Cookstoves and Implications for Metrics Useful in Setting International Test Standards. *Environ. Sci. Technol.* **2012**, *46* (19), 10827–10834.
- (6) Just, B.; Rogak, S.; Kandlikar, M. Characterization of Ultrafine Particulate Matter from

- Traditional and Improved Biomass Cookstoves. *Environ. Sci. Technol.* **2013**, *47* (7), 3506–3512.
- (7) Preble, C. V.; Hadley, O. L.; Gadgil, A. J.; Kirchstetter, T. W. Emissions and Climate-Relevant Optical Properties of Pollutants Emitted from a Three-Stone Fire and the Berkeley-Darfur Stove Tested under Laboratory Conditions. *Environ. Sci. Technol.* **2014**, *48* (11), 6484–6491.
- (8) Tryner, J.; Willson, B. D.; Marchese, A. J. The effects of fuel type and stove design on emissions and efficiency of natural-draft semi-gasifier biomass cookstoves. *Energy for Sustainable Development* **2014**, *23*, 99–109.
- (9) Sutar, K. B.; Kohli, S.; Ravi, M. R.; Ray, A. Biomass cookstoves: A review of technical aspects. *Renewable and Sustainable Energy Reviews* **2015**, *41*, 1128–1166.
- (10) Still, D.; Bentson, S.; Li, H. Results of Laboratory Testing of 15 Cookstove Designs in Accordance with the ISO/IWA Tiers of Performance. *EcoHealth* **2015**, *12* (1), 12–24.
- (11) MacCarty, N.; Still, D.; Ogle, D. Fuel use and emissions performance of fifty cooking stoves in the laboratory and related benchmarks of performance. *Energy for Sustainable Development* **2010**, *14* (3), 161–171.
- (12) Flagan, R. C.; Seinfeld, J. H. *Fundamentals of Air Pollution Engineering*; Hall, P., Ed.; Englewood Cliffs, New Jersey 07632, 1988.
- (13) Hawley, B.; Volckens, J. Proinflammatory effects of cookstove emissions on human bronchial epithelial cells. *Indoor Air* **2012**, *23* (1), 4–13.
- (14) Stoeger, T.; Reinhard, C.; Takenaka, S.; Schroepel, A.; Karg, E.; Ritter, B.; Heyder, J.; Schulz, H. Instillation of Six Different Ultrafine Carbon Particles Indicates a Surface Area Threshold Dose for Acute Lung Inflammation in Mice. *Environ Health Perspect*

- 2005**, *114* (3), 328–333.
- (15) Warheit, D. B.; Webb, T. R.; Reed, K. L.; Frerichs, S.; Sayes, C. M. Pulmonary toxicity study in rats with three forms of ultrafine-TiO<sub>2</sub> particles: Differential responses related to surface properties. *Toxicology* **2007**, *230* (1), 90–104.
- (16) Oberdörster, G.; Oberdörster, E.; Oberdörster, J. Nanotoxicology: An Emerging Discipline Evolving from Studies of Ultrafine Particles. *Environ Health Perspect* **2005**, *113* (7), 823–839.
- (17) Gurr, J.-R.; Wang, A. S. S.; Chen, C.-H.; Jan, K.-Y. Ultrafine titanium dioxide particles in the absence of photoactivation can induce oxidative damage to human bronchial epithelial cells. *Toxicology* **2005**, *213*, 66–73.
- (18) Brown, D. M.; Wilson, M. R.; MacNee, W.; Stone, V.; Donaldson, K. Size-Dependent Proinflammatory Effects of Ultrafine Polystyrene Particles: A Role for Surface Area and Oxidative Stress in the Enhanced Activity of Ultrafines. *Toxicology and Applied Pharmacology* **2001**, *175* (3), 191–199.
- (19) The Water Boiling Test Version 4.2.3: Cookstove Emissions and Efficiency in a Controlled Laboratory Setting. The Global Alliance for Clean Cookstoves March 18, 2014, pp 1–89.
- (20) Levin, E. J. T.; McMeeking, G. R.; Carrico, C. M.; Mack, L. E.; Kreidenweis, S. M.; Wold, C. E.; Moosmüller, H.; Arnott, W. P.; Hao, W. M.; Collett, J. L., Jr.; et al. Biomass burning smoke aerosol properties measured during Fire Laboratory at Missoula Experiments (FLAME). *J. Geophys. Res.* **2010**, *115* (D18), D18210–D18215.
- (21) Hand, J. L.; Kreidenweis, S. M. A New Method for Retrieving Particle Refractive Index and Effective Density from Aerosol Size Distribution Data. **2002**, *36* (10), 1012–1026.

- (22) Taylor, J. R. *An Introduction To Error Analysis*, Second. McGuire, A., Ed.; University Science Books: Sausalito, CA, 1997.
- (23) Wang, Y.; Sohn, M. D.; Wang, Y.; Lask, K. M.; Kirchstetter, T. W.; Gadgil, A. J. How many replicate tests are needed to test cookstove performance and emissions? — Three is not always adequate. *Energy for Sustainable Development* **2014**, *20*, 21–29.
- (24) Hays, M. D.; Fine, P. M.; Geron, C. D.; Kleeman, M. J.; Gullett, B. K. Open burning of agricultural biomass: Physical and chemical properties of particle-phase emissions. *Atmospheric Environment* **2005**, *39* (36), 6747–6764.
- (25) Hosseini, S.; Li, Q.; Cocker, D.; Weise, D.; Miller, A.; Shrivastava, M.; Miller, J. W.; Mahalingam, S.; Princevac, M.; Jung, H. Particle size distributions from laboratory-scale biomass fires using fast response instruments. *Atmos. Chem. Phys.* **2010**, *10* (16), 8065–8076.
- (26) Hinds, W. C. *Aerosol Technology*, Second. John Wiley & Sons, 2012.
- (27) Hofmann, W. Modelling inhaled particle deposition in the human lung—A review. *Journal of Aerosol Science* **2011**, *42* (10), 693–724.

## **SUPPORTING INFORMATION**

### **Reducing ultrafine particle emissions using air injection in wood-burning cookstoves**

Vi H. Rapp\*†, Julien J. Caubel†‡, Daniel L. Wilson†‡, Ashok J. Gadgil†¶

†Environmental Technologies Area, Lawrence Berkeley National Laboratory, Berkeley, California 94720, United States

‡Department of Mechanical Engineering, University of California, Berkeley, Berkeley, California 94720, United States

¶Department of Civil and Environmental Engineering, University of California, Berkeley, Berkeley, California 94720, United States

\*Corresponding Author: Vi Rapp, Environmental Technologies Area, Lawrence Berkeley National Laboratory, 1 Cyclotron Road MS90R2121, Berkeley, California 94720, United States; Phone: +01(510)495-2035; Fax: +01(510)486-4089; E-mail: vhrapp@lbl.gov

Number of pages: 16

Number of tables: 4

Number of figures: 4

**Accepted June 2016 to Environmental Science and Technology**

**DOI: 10.1021/acs.est.6b01333**

## S-1 MATERIALS AND METHODS

**Three-stone Fire (TSF).** The TSF in this study was comprised of three stones of similar size arranged on a tray in a triangular configuration, as shown in Figure S1. The stones were placed on a tray that contained sand approximately 5 cm deep to better mimic the thermal conductivity of the ground that is typical of cooking in Darfur, as well as to prevent heat transfer from the stove to the scale. The circumference of the stones was arranged such that the lowest point of the round-bottomed Darfuri pot was approximately 10 cm above the sand, as described in the WBT protocol. Fuel wood sticks were arranged in a radial pattern in order to keep the fire directly under the pot. This fire tending method is similar to the “carefully tended” mode described by Jetter et al. (2012)<sup>1</sup>.



**Figure S1.** Three-stone fire arrangement with Darfur pot.

**Berkeley Darfur Stove (BDS).** The BDS was developed at Lawrence Berkeley National Laboratory (LBNL) and the University of California, Berkeley to aid internally displaced populations from the Sudan civil war living in displacement camps in Darfur. The design reduces the amount of wood needed for cooking through increased thermal efficiency compared to

cooking over a TSF. The design in this study (version 14) was adapted from the India's Tara Stove and modified to reduce manufacturing cost, simplify assembly, increase life of the stove, and meet the cultural and regional cooking requirements of Darfuri women<sup>2</sup>. The BDS was designed to interface and operate with Darfuri style pots and is comprised of a cast iron grate, a stainless steel firebox, and other components made from mild steel sheet metal. The design allows for efficient flat shipping to Darfur where they are assembled into stoves. Since 2009, Potential Energy, non-profit organization, has distributed and sold over 40,000 Berkeley Darfur Stoves (<http://www.potentialenergy.org/>). Additional details about the BDS can be found in Preble et al. (2014) and Jetter et al. (2012)<sup>1,2</sup>.

**Berkeley Umbrella Stove (BUS).** The Berkeley Umbrella Stove (BUS), Figure S1, incorporates an umbrella-shaped air injection manifold into the BDS firebox with downward-facing jets that promote mixing and complete combustion in the gas-phase combustion zone. During operation, compressed air from a cylinder was regulated using a 2-stage regulator and then flowed through a rotameter (measuring volumetric flow rate) before passing through the central column into the umbrella-shaped manifold. Releasing the air from the high-pressure cylinder cools it substantially. To bring the air temperature back to room temperature, it was passed through a long thin copper tubing immersed in a bucket of warm water. The pressure at the inlet to the stove manifold with the rotometer wide open, to reduce flow restrictions, was measured to be approximately 492 Pa (0.07 psi) at a flow rate of 56.6 LPM (2 CFM), within the design limits for use with a small (2-4 Watt) blower.

The umbrella is made of two 6-inch (15.24 cm) diameter stainless steel plates, 1/16-inches (1.588 mm) thick, welded to a stainless steel ring 1/2-inch (1.27 cm) tall. Located on the bottom surface of the umbrella are 42 1/8-inch (3.175 mm) diameter holes that are equally spaced in a

concentric pattern. During operation, air (supplied from a cylinder of compressed air) passes through a central column and then into the umbrella-shaped manifold. Air is then ejected out the 1/8-inch (3.175 mm) diameter holes into the gas-phase combustion zone in the firebox. The pot sits about 0.4-inches (10 mm) above the umbrella.

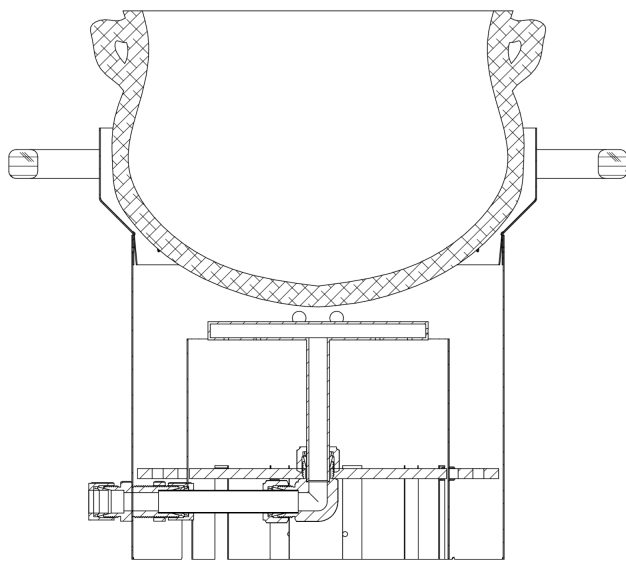


**Figure S-2.** Cross-sectional view of the Berkeley Umbrella Stove looking from the front.

The bottom surface of the manifold contains 42 downward-facing jets to promote mixing and complete combustion in the gas-phase combustion zone.

**Berkeley Shower Stove (BSS).** The Berkeley Shower Stove (BSS), Figure S2, employs up to eight interchangeable stainless-steel nozzles, or “shower-heads,” to inject air over the firebox wall into the gas-phase combustion zone. The air injection manifold is located below the stove grate and was designed to avoid the radiation shielding effect experienced with the BUS. Additionally, this stove and manifold were designed to allow for rapid parametric investigation of air injection geometries that improve thermal performance while significantly reducing emissions. The pressure at the inlet to the stove manifold with the rotometer wide open, to reduce

flow restrictions, was measured to be approximately 17.2 kPa (2.5 psi) at a flow rate of 42.5 LPM (1.5 CFM).

The manifold is made of two 10-inch (25.4 cm) diameter stainless steel plates welded to a stainless steel ring 2-inches (5 cm) in height. The 10-inch (25.4 cm) diameter plates are 1/4-inch (6.35 mm) thick to allow for drilling and tapping for the nozzles, while the 2-inch (5.08 cm) tall ring is 1/16-inch (1.588 mm) thick. Before air reaches the manifold and nozzles, it travels through 2-ft (61 cm) of 1/4-inch (6.35 mm) coiled copper tubing located directly below the grate to preheat the air. Eight stainless steel nozzles, oriented radially around the firebox, are used for air injection. Each nozzle has an inner diameter of 0.18-inches (4.572 mm) (0.035-inch, 0.889 mm, wall thickness with 0.25-inch, 6.35 mm, outer diameter), protrudes 3.5-inches (8.89 mm) above the grate and the peak height of the nozzle is approximately 2 inches (5 cm) below the pot. The two nozzles at the rear of the firebox are angled towards each other to prevent hot gases and flames from exiting out the fuel magazine feed towards the stove operator. All the nozzle tips are angled approximately 45 degrees downwards from the horizontal plane.

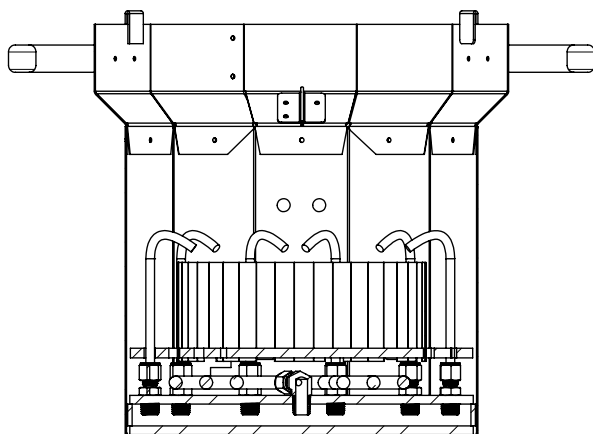


**Figure S3.** Cross-sectional view of the Berkeley Shower Stove looking from the front. The nozzles protrude through the stove grate to inject air over the firebox into the gas-phase

combustion zone. The air manifold sits below the grate and air is preheated through the copper tubing before entering the manifold and being distributed to the 8 nozzles (only 6 are shown).

**Experimental Setup.** All experiments were conducted in the Lawrence Berkeley National Laboratory cookstove research facility. A detailed schematic of the gravimetric PM sample and the real-time aerosol sample setup is shown in Figure S4. Ultra zero air (oxygen 19.5% - 23.5%, water < 2 ppm, hydrocarbons < 0.1 ppm, CO<sub>2</sub> < 0.5 ppm, CO < 0.5 ppm) from a compressed cylinder was used to dilute the real-time aerosol sampling line before reaching the particle instruments. Dilution ratio was calculated using measured mass flow rates and validated using the ratio of CO<sub>2</sub> concentrations before and after dilution in the sample line. Conductive tubing was used for all particle sampling lines and flow rates of emissions extracted from the exhaust system and sampled during cookstove testing were chosen to ensure isokinetic flow for the gravimetric PM system. Emissions for the real-time aerosol particle instruments were sampled anisokinetically. Particle number concentration and size distribution measured at 1 Hz sampling rate were measured using a TSI 3330 Optical Particle Sizer (OPS) and a TSI 3091 Fast Mobility Particle Sizer (FMPS). The FMPS measured number concentration and size distribution of particles between 5 nm and 300 nm, while the OPS measured number concentration and size distribution of particles between 300 nm and 10 μm.

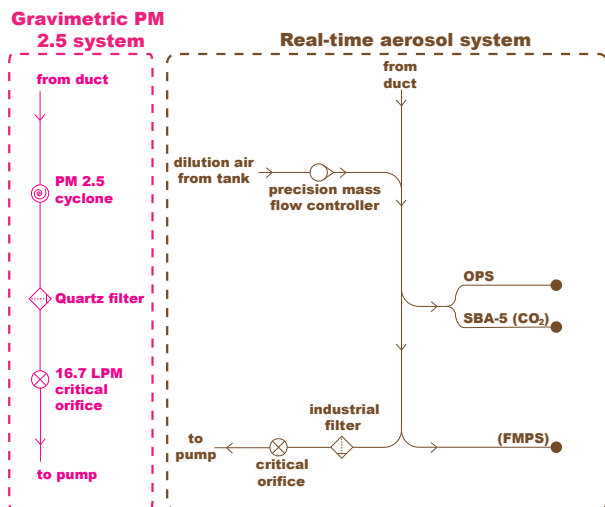


**Figure S4.** Schematic of the Lawrence Berkeley National Laboratory cookstove research testing facility.

Moisture content of the fuel wood was measured using a Delmhorst J-2000 moisture meter (calibrated using an oven-drying technique). A thermocouple data logger was used to measure water, duct, and ambient temperature. An Energy Conservatory Automated Performance Testing System (APT-8) equipped with eight pressure sensors and a relative humidity sensor was used to measure duct humidity, differential pressure between the room and various locations in the exhaust duct, and differential pressure across an adjustable iris in the exhaust duct for determining duct flow rate. Real time fuel consumption and water evaporation were measured with an electronic platform scale (64 kg capacity and 0.1 g resolution) and a small scale was used for measuring unburned wood, char, and water loss from boiling (6 kg capacity and 0.1 g resolution). During each experiment, all exhaust sample flows (gaseous and aerosol) were periodically validated with a primary airflow calibrator (a Gilian Gilibrator that meets National Institute for Occupational Safety and Health (NIOSH) accuracy requirements).

At the beginning of each experiment day, all instruments were calibrated for offset using ultra high purity (99.999%) nitrogen for gas analyzers and ultra-zero air for particle instruments.

The CAI-600 gas analyzer was also calibrated for span using 1000 ppm CO and 5000 ppm CO<sub>2</sub> calibration gases, and room air for O<sub>2</sub> calibration (assuming a constant ambient concentration of 21.0%). At the end of each experiment day, calibration of the instruments was validated to ensure accuracy.

**Experimental Procedure.** The fire was started using 15 g of untreated pine wood shavings (commercially sold in pet shops for hamster bedding) and 60 g of Douglas-fir kindling (cut into 0.5 cm x 0.5 cm x 8 cm pieces). The fire was then built up by adding Douglas-fir fuel-wood pieces (2 cm x 2 cm x 20 cm in size) to heat the water from ambient temperature to boiling (approximately 99°C for experiments presented in this paper). Both the kindling and the fuel-wood were untreated and harvested from a single Douglas-fir tree and stored in a dry location for at least 1 year prior to the experiments. The moisture content of the wood ranged from 6% to 8% on a wet basis.

For all stove tests, the operator added fuel-wood to the fire at a rate that maintained a constant 3000 ppm carbon dioxide (CO<sub>2</sub>) concentration in the exhaust duct. We selected this CO<sub>2</sub> concentration, and the corresponding firepower (~ 5 kW), because it represents an achievable and maintainable firepower from a TSF that will successfully bring 5 L of water to a boil. Due to the unstable nature of the combustion in the TSF, duct CO<sub>2</sub> concentrations, and the TSF's firepower, varied much more than when testing the engineered stoves.

In order to identify the optimal configuration for the BSS, parametric tests varying nozzle height, number, and position were conducted. The 4 replicate tests presented in this study are a subset from the larger parametric study. When calculating relevant performance and emissions metrics, it was found that the BSS performs very consistently and that the 4 replicate tests

provided confidence intervals comparable (and often smaller than) the other stove types. Consequently, no further replicate tests were conducted.

**Data Analysis.** Due to variation in the initial temperature of the water, the temperature-corrected time to boil is used for comparing boiling time of each experiment. The temperature-corrected time to boil is determined using,

$$\Delta t_{\text{corr}} = \Delta t \cdot \frac{75}{T_f - T_i} \quad (S1)$$

where  $\Delta t$  is the measured time to boil,  $T_f$  is the final boiling temperature of the water, and  $T_i$  is the initial temperature of the water. Equation S1 standardizes the measured boiling time by assuming a 75°C water temperature change (from 25°C to 100°C)<sup>3</sup>.

The modified combustion efficiency (MCE) was calculated using,

$$\text{MCE} = \frac{\Delta \text{CO}_2}{\Delta \text{CO}_2 + \Delta \text{CO}} \quad (S2)$$

where  $\Delta \text{CO}_2$  is the difference between the mean duct concentration and background concentration of carbon dioxide measured in ppmv (parts per million by volume) and  $\Delta \text{CO}$  is the difference between the mean duct concentration and background concentration (typically zero) of carbon monoxide measured in ppmv.

Total particle mass generated by the stove in milligrams per cubic meter was determined using,

$$\text{PM}_{2.5\_stove} \left[ \frac{\text{mg}}{\text{m}^3} \right] = \frac{\text{PM}_{2.5\_filter} [\text{g}]}{t_{\text{test}} [\text{s}] \times Q_{\text{sample}} \left[ \frac{\text{m}^3}{\text{s}} \right]} \quad (S3)$$

where  $PM_{2.5\_filter}$  is the total mass of  $PM_{2.5}$  measured from a gravimetric filter,  $t_{test}$  is the total time of the test or total time the filter was used for sampling, and  $Q_{sample}$  is the flow rate of the sample through the filter.

The total particle number size distribution and generation rate is calculated using  $dN/d\log(D_p)$  data from the FMPS and OPS, where  $dN$  is the PM concentration in units of number of particles per cubic centimeter of air per particle size bin, and  $d\log(D_p)$  is the logarithmic width of the corresponding particle size bin in log nanometers. Each instrument has a constant logarithmic bin width throughout their measurement range.

The total particle number distribution generated over the course of a test  $dN_t/d\log(D_p)$  is calculated for each particle bin using,

$$\frac{dN_t}{d\log D_p} = \sum_{t=0}^{t_{test}} \left( \frac{dN}{d\log D_p} \right)_t \cdot \overline{DR} \cdot \overline{Q}_{duct} \cdot \Delta t \quad (S4)$$

where  $t_{test}$  is the duration of the test in seconds,  $\left( \frac{dN}{d\log D_p} \right)_t$  is the particle number concentration at time 't',  $\overline{DR}$  is the mean dilution ratio in the sampling system over the course of the test,  $\overline{Q}_{duct}$  is the mean volumetric flow rate in the duct, and  $\Delta t$  is the sampling interval, equal to 1 second for all instruments. When applied to all particle bins over each instrument's measurement range, this equation yields a distribution of the total number of particles generated by the stove over the test duration as a function of particle diameter.

The particle number generation rate over a specified particle diameter range,  $\dot{N}$ , is calculated at each sampling interval using,

$$\dot{N} = \sum_{d=d_i}^{d=d_f} \left( \frac{dN}{d\log D_p} \right)_d \cdot \overline{DR} \cdot \overline{Q}_{duct} \cdot d\log(D_p) \quad (S5)$$

where  $d_f$  and  $d_i$  are the upper and lower bounds of the particle diameter range in nm and  $d\log(D_p)$  is the instrument-specific constant bin width cited above. By applying this equation at each sampling interval over the test duration, it is possible to calculate the total number generation rate of particles within a specified particle diameter range as a function of time. Equation (S5) can be normalized by the equivalent mass of dry fuel consumed during the test. This equivalent mass more accurately represents the energy content of the fuel consumed by accounting for the energy required to evaporate the moisture in the fuel and the amount of char remaining unburned at the end of the test<sup>3</sup>, as shown in Equation (S6).

$$m_{fcd} = \frac{m_{fcm}(\text{LHV}(1 - \text{MC}) - \text{MC}(4.186(T_b - T_a) + 2257)) - \Delta m_{\text{char}} \cdot \text{LHV}_{\text{char}}}{\text{LHV}} \quad (\text{S6})$$

where  $m_{fcd}$  is the equivalent dry fuel consumed (Kg),  $m_{fcm}$  is the moist fuel consumed (Kg), LHV is the lower heating value of the dry fuel (KJ/Kg), MC is the moisture content of the fuel,  $T_b$  is the boiling temperature of the water (in °C),  $T_a$  is the ambient temperature of the water (in °C),  $m_{\text{char}}$  is the char remaining (Kg), and  $\text{LHV}_{\text{char}}$  is the lower heating value of the char (KJ/Kg).

## RESULTS AND DISCUSSION

**Performance Metrics.** Tables S1 through S4 provide WBT 4.2.3<sup>3</sup> calculated metrics for individual stove tests.

Table S1. Calculated metrics from the WBT 4.2.3<sup>3</sup> protocol for individual Three-Stone Fire (TSF) tests.

	TSF01	TSF02	TSF03	TSF04	TSF05	TSF06	TSF07	TSF08	TSF09	TSF10
Time to boil [min]	34	26	27	22	27	31	41	35	33	34
Corrected time to boil [min]	33	26	26	24	31	32	39	38	35	34
Equivalent dry wood consumed [g]	563	478	497	444	532	430	572	471	602	544
Exhaust carbon concentration [ppm]	1987	2528	2721	2889	2583	2506	1913	1881	2493	2152
Total carbon in exhaust [g/m <sup>3</sup> ]	0.94	1.18	1.26	1.32	1.19	1.15	0.91	0.87	1.13	1.01
CO emission factor [g CO/kg fuel]	47.25	38.01	45.40	46.32	31.20	29.20	49.45	46.81	39.78	56.22
PM <sub>2.5</sub> emission factor [g PM <sub>2.5</sub> /kg fuel]	2.43	3.08	2.70	4.74	3.69	3.43	3.04	2.29	3.82	2.13
CO Total mass emitted [g]	24.97	16.41	20.52	18.63	15.64	10.41	26.66	21.19	23.09	29.57
PM <sub>2.5</sub> Total mass emitted [g]	1.29	1.33	1.22	1.91	1.85	1.22	1.64	1.04	2.22	1.12
Average fuel burn rate [g/min]	16.40	18.50	18.74	20.56	19.51	13.80	14.03	13.38	18.43	15.91
Firepower [W]	5128	5786	5862	6432	6102	4316	4388	4183	5766	4976
Combustion Efficiency	96%	97%	96%	96%	97%	97%	96%	96%	97%	95%
Thermal Efficiency	21%	23%	23%	22%	20%	27%	24%	24%	19%	23%
Cooking energy CO emissions [g/MJ <sub>del</sub> ]	11.14	8.04	9.40	10.10	7.66	4.72	10.50	9.86	10.73	12.67
Cooking energy PM <sub>2.5</sub> emissions [mg/MJ <sub>del</sub> ]	574.05	651.07	558.20	1033.7 1	905.33	553.22	646.35	481.86	1030.9 1	480.87
CO emission rate [g/min]	0.73	0.66	0.79	0.89	0.58	0.34	0.67	0.61	0.72	0.87
PM <sub>2.5</sub> emission rate [g/min]	37.85	53.18	46.87	90.79	68.43	39.39	41.02	29.60	69.30	33.00

Table S2. Calculated metrics from the WBT 4.2.3<sup>3</sup> protocol for individual Berkeley Darfur Stove (BDS) tests.

	BDS01	BDS02	BDS03	BDS04	BDS05	BDS06	BDS07	BDS08	BDS09	BDS10
Time to boil [min]	21	18	18	19	17	15	19	19	19	18
Corrected time to boil [min]	19	18	18	19	17	16	18	18	20	19
Equivalent dry wood consumed [g]	309	313	312	320	284	277	321	318	283	288
Exhaust carbon concentration [ppm]	2015	2177	2380	2235	2350	2385	2112	2148	2111	2180
Total carbon in exhaust [g/m <sup>3</sup> ]	0.98	1.04	1.11	1.04	1.11	1.13	1.01	1.02	0.99	1.03
CO emission factor [g CO/kg fuel]	29.54	41.23	39.45	43.86	40.91	40.64	66.91	52.50	60.89	56.60
PM <sub>2.5</sub> emission factor [g PM <sub>2.5</sub> /kg fuel]	3.86	4.16	4.14	4.51	5.49	5.21	5.66	5.47	4.80	5.15
CO Total mass emitted [g]	8.76	12.46	11.81	13.56	11.14	10.89	20.70	16.40	16.62	15.75
PM <sub>2.5</sub> Total mass emitted [g]	1.14	1.26	1.24	1.39	1.50	1.40	1.75	1.71	1.31	1.43
Average fuel burn rate [g/min]	14.61	16.98	17.38	16.59	17.08	18.61	17.16	16.85	14.70	16.30
Firepower [W]	4569	5310	5437	5188	5341	5822	5367	5270	4598	5098
Combustion Efficiency	97%	96%	97%	96%	96%	96%	94%	95%	95%	95%
Thermal Efficiency	36%	34%	34%	33%	34%	33%	32%	33%	36%	34%
Cooking energy CO emissions [g/MJ <sub>del</sub> ]	4.14	6.26	6.00	6.83	6.18	6.28	10.60	8.41	8.66	8.65
Cooking energy PM <sub>2.5</sub> emissions [mg/MJ <sub>del</sub> ]	540.74	631.39	629.34	702.21	829.59	804.93	896.68	876.08	683.42	786.62
CO emission rate [g/min]	0.42	0.69	0.69	0.71	0.70	0.78	1.15	0.91	0.87	0.93
PM <sub>2.5</sub> emission rate [g/min]	54.49	69.77	72.87	73.35	93.52	99.76	97.29	94.88	69.01	84.26

Table S3. Calculated metrics from the WBT 4.2.3<sup>3</sup> protocol for individual Berkeley Umbrella

Stove (BUS) tests.

	BUS01	BUS02	BUS03	BUS04	BUS05	BUS06	BUS07	BUS08	BUS09	BUS10
Time to boil [min]	23	25	22	20	22	21	20	20	21	19
Corrected time to boil [min]	22	25	21	22	21	21	21	20	23	19
Equivalent dry wood consumed [g]	367	373	327	326	395	364	351	393	421	343
Exhaust carbon concentration [ppm]	2163	1863	2220	2348	2428	2487	2521	2578	2431	2466
Total carbon in exhaust [g/m <sup>3</sup> ]	1.04	0.89	1.06	1.09	1.15	1.17	1.17	1.22	1.14	1.16
CO emission factor [g CO/kg fuel]	31.22	22.71	53.37	42.19	24.13	39.49	35.07	39.94	31.25	41.72
PM <sub>2.5</sub> emission factor [g PM <sub>2.5</sub> /kg fuel]	2.48	2.63	2.34	3.36	1.75	2.39	2.61	2.29	2.80	2.68
CO Total mass emitted [g]	11.04	8.39	16.62	13.31	9.32	13.93	11.91	15.38	13.29	13.81
PM <sub>2.5</sub> Total mass emitted [g]	0.88	0.97	0.73	1.06	0.68	0.84	0.88	0.88	1.19	0.89
Average fuel burn rate [g/min]	15.68	15.04	15.22	16.49	17.95	17.13	17.47	19.21	19.82	18.34
Firepower [W]	4905	4703	4760	5157	5613	5358	5465	6007	6199	5737
Combustion Efficiency	97%	98%	95%	96%	98%	97%	97%	97%	97%	96%
Thermal Efficiency	30%	28%	31%	29%	28%	30%	29%	29%	24%	31%
Cooking energy CO emissions [g/MJ <sub>del</sub> ]	5.26	4.22	8.67	7.47	4.47	6.70	6.25	7.21	6.88	6.92
Cooking energy PM <sub>2.5</sub> emissions [mg/MJ <sub>del</sub> ]	418.12	489.18	380.72	594.72	323.75	404.66	464.19	412.83	617.13	443.40
CO emission rate [g/min]	0.48	0.35	0.79	0.70	0.44	0.66	0.60	0.77	0.63	0.77
PM <sub>2.5</sub> emission rate [g/min]	38.16	40.54	34.76	55.78	32.17	40.06	44.22	44.05	56.77	49.19

Table S4. Calculated metrics from the WBT 4.2.3<sup>3</sup> protocol for individual Berkeley Shower Stove (BSS) tests.

	BSS01	BSS02	BSS03	BSS04
Time to boil [min]	21	20	20	19
Corrected time to boil [min]	19	19	18	18
Equivalent dry wood consumed [g]	333	317	339	333
Exhaust carbon concentration [ppm]	2163	2132	2336	2343
Total carbon in exhaust [g/m <sup>3</sup> ]	1.04	1.02	1.13	1.12
CO emission factor [g CO/kg fuel]	18.59	18.16	17.56	10.78
PM2.5 emission factor [g PM2.5/kg fuel]	1.22	1.62	1.64	1.50
CO Total mass emitted [g]	6.05	5.59	5.88	3.51
PM2.5 Total mass emitted [g]	0.40	0.50	0.55	0.49
Average fuel burn rate [g/min]	15.88	15.87	17.27	17.52
Firepower [W]	4968	4965	5401	5479
Combustion Efficiency	98%	98%	98%	99%
Thermal Efficiency	35%	35%	33%	33%
Cooking energy CO emissions [g/MJ <sub>del</sub> ]	2.81	2.69	2.78	1.69
Cooking energy PM2.5 emissions [mg/MJ <sub>del</sub> ]	184.07	239.54	259.42	235.13
CO emission rate [g/min]	0.30	0.29	0.31	0.18
PM2.5 emission rate [g/min]	19.84	26.23	28.84	25.77

## REFERENCE

- (1) Jetter, J.; Zhao, Y.; Smith, K. R.; Khan, B.; Yelverton, T.; DeCarlo, P.; Hays, M. D. Pollutant Emissions and Energy Efficiency under Controlled Conditions for Household Biomass Cookstoves and Implications for Metrics Useful in Setting International Test Standards. *Environ. Sci. Technol.* **2012**, *46* (19), 10827–10834.
- (2) Preble, C. V.; Hadley, O. L.; Gadgil, A. J.; Kirchstetter, T. W. Emissions and Climate-Relevant Optical Properties of Pollutants Emitted from a Three-Stone Fire and the Berkeley-Darfur Stove Tested under Laboratory Conditions. *Environ. Sci. Technol.* **2014**, *48* (11), 6484–6491.
- (3) The Water Boiling Test Version 4.2.3: Cookstove Emissions and Efficiency in a Controlled Laboratory Setting. The Global Alliance for Clean Cookstoves March 18, 2014, pp 1–89.